300,000-year-old wooden tools from Gantangqing, southwest China

Xing Gao (gaoxing@ivpp.ac.cn)
Chinese Academy of Sciences

Jian-Hui Liu
Yunnan Institute of Cultural Relics and Archeology

Qi-Jun Ruan
Yunnan Institute of Cultural Relics and Archeology

Junyi Ge
Key Laboratory of Vertebrate Evolution and Human Origins of Chinese Academy of Sciences, Institute of Vertebrate Paleontology and Paleoanthropology, Beijing, 100044，China https://orcid.org/0000-0002-4569-2915

Yongjiang Huang
Kunming Institute of Botany, Chinese Academyof Sciences

Jia Liu
CAS Key Laboratory of Tropical Forest Ecology, Xishuangbanna Tropical Botanical Garden, Chinese Academy of Sciences

Shufeng Li
Xishuangbanna Tropical Botanical Garden, Chinese Academy of Sciences

Ying Guan
Key Laboratory of Vertebrate Evolution and Human Origins of Chinese Academy of Sciences, Institute of Vertebrate Paleontology and Paleoanthropology, Beijing, 100044，China

Hui Shen
Institute of Vertebrate Palaeontology and Palaeoanthropology, Chinese Academy of Sciences

Yuan Wang
Institute of Vertebrate Paleontology and Paleoanthropology

Thomas Stidham
Institute of Vertebrate Paleontology and Paleoanthropology, Chinese Academy of Sciences

Chenglong Deng
State Key Laboratory of Lithospheric Evolution, Institute of Geology and Geophysics, Chinese Academy of Sciences https://orcid.org/0000-0003-1848-3170

Shenghua Li
Department of Earth Sciences, The University of Hong Kong

Fei Han
Yunnan University

Bo Li
University of Wollongong https://orcid.org/0000-0003-4186-4828
Robin Dennell
University of Exeter

Biological Sciences - Article

Keywords: Palaeolithic Wooden Implements, Digging Sticks, Sub-aquatic Plants, Sub-surface Plant Foods, Middle Pleistocene

Posted Date: February 16th, 2021

DOI: https://doi.org/10.21203/rs.3.rs-226285/v1

Abstract

Early Palaeolithic wooden implements are exceptionally rare. The best known are the spears and throwing sticks from Schöningen, Germany dated to ca. 300–330 thousand years (kyr) ago [1,2] and the 171-kyr old digging sticks from Poggetti Vecchi, Italy [3]. Here, we report a unique assemblage of 35 wooden implements from the site of Gantangqing, southwestern China, which was found associated with stone tools, antler soft hammers and cut-marked bones, and is dated to ca. 361–250 kyr at 95% probability. The wooden implements include digging sticks and complete, small, hand-held pointed tools. The tips of several had starch grains of plants with starch-rich rhizomes. We suggest that most of these tools were used for digging the rhizomes of sub-aquatic plants on the edges of an ancient lake. This discovery provides the earliest tangible evidence for the exploitation of sub-surface plant foods in the Middle Pleistocene. It also highlights the probable role of plant foods (especially underground storage organs [USOs]) in sub-tropical and tropical environments in which a wide variety of edible plants were available, and implies that hominins had a detailed knowledge of which plants, and which parts of plants, were edible. These tools also show that organic materials played an important role in Middle Pleistocene technology, and the sophistication of many of these tools off-sets the seemingly “primitive” design of stone tools in the East Asian Early Palaeolithic.

Main Text

The site of Gantangqing (GTQ) is located ca. 9.4 km northeast of the administrative centre of Jiangchuan county, at 24°18'26.76"N, 102°50'48.20"E, with an altitude of ~1836 m. It is situated on the southern margin of the Lake Fuxian basin, ca. 5.6 km from Lake Fuxian (Fig. 1). The Lake Fuxian basin is a fault-depression formed by the uplift of the central Yunnan plateau from the late Neogene to early Pleistocene, located in the Xiaojiang fault zone [4,5] (see Supplementary Information for details). The deposits at GTQ accumulated in the lakeside piedmont zone of ancient Lake Fuxian and have now eroded into a small slope (Fig. 2). The site is named after a narrow river called Gantangqing that runs from south to north from the foothills. Today, the climate is strongly monsoonal, with rainfall averaging ca. 900 mm p.a. that mostly falls between July and September and with annual temperature averaging ca. 20 °C.

The site was discovered in 1984 and first excavated in 1989, when numerous lithic materials and faunal remains were found[6,7]. Two new excavations of four trenches (T1–T4) were conducted from October 2014 to February 2015 (T1 and T2) and October 2018 to May 2019 (T3 and T4) that exposed an area of 64 m^2, reaching depths from 3.5 to 7 meters, respectively (Fig. 2a, Extended Data Figs. 1 and 2). Stone artefacts, wooden implements, faunal and floral remains were recovered from all the trenches, and geological and geochronological researches were conducted. All materials discussed in this paper came from the new excavations.

Geological and stratigraphic observations indicate that the sedimentary sequence at the site is the result of lake-shore lacustrine/fluvial deposition associated with the ancient Fuxian Lake. The sedimentary sequence underneath modern plough soil can be divided into three major units (I, II and III) that are unconformably bedded from top to bottom (Fig. 2c, Supplementary Information Section 1). Unit I comprises red soils at the top and greyish-yellow clay interbedded with yellowish sand at the bottom. Grain size analysis suggests a lacustrine-fluvial origin of the sediments from Unit I (Supplementary Information Section 1). Unit II consists primarily of blueish-grey lacustrine deposits. Unit III, at the base of the section, is Cambrian sandy shale. Artefacts were recovered from Unit I only. Our new excavations revealed the middle and lower parts of Unit I and the upper part of Unit II in all trenches (Fig. 2c). The sedimentary features and stratigraphic sequence are generally similar across trenches (Extended Data Fig. 2). A total of 20 stratigraphic layers were recognised (Fig. 2d, Supplementary Table 1), with lateral variations and discontinuities, as well as unconformities. As a result, different numbers of layers were identified in different trenches; T1 and T2 have the complete sequence of 20 layers (Layers 1–20), T3 has 16 layers and T4 has 11 layers (Supplementary Table 1). Stratigraphic correlation was achieved by field observations of sedimentary characteristics and morphological features (Supplementary Table 1). The wooden and other implements (see Fig. 3, Extended Data Figs. 3–10, Supplementary Information Sections 3, 4 and 5), and numerous faunal and floral remains, were recovered from Layers 10–18 (Fig. 2) of Unit I. Organic preservation was exceptional in the waterlogged deposits of Layers 14–17; most fossils and artefacts are fresh, with no or very little sign of weathering. Wooden artefacts were usually intact when found (Extended Data Figs. 1, 4–9). No obvious orientation was observed, and all material appears to have been buried rapidly but under gentle conditions of deposition.

We established a robust chronologic framework for the site based on palaeomagnetism, optical dating and electron spin resonance (ESR) dating (see Methods and Supplementary Information Section 2). Palaeomagnetic analysis indicated that all samples from Unit I had a normal polarity; faunal evidence (Supplementary Information Sections 6 and 7) indicates that this is most likely the Brunhes Normal Chron. The layers of Unit I were dated by the coupled U-series and ESR dating of dental fragments from a fossil tooth recovered from Layer 13 in T4, as well as optical dating of potassium-rich feldspar (K-feldspar) from 23 sediment samples (Fig. 2d and Extended Data Fig. 2), including 6 from T1 (Layers 13–18), 3 from T3 (Layers 10, 14–16) and 14 from T4 (Layers 7–15). The optical and the ESR/U-series dating results range from ~200 to ~400 kyr (at 95% confidential interval), which are broadly consistent with each other and stratigraphically coherent (Fig. 2d, e). The equivalent dose (D_e) distributions of individual feldspar grains show minimal evidence for large-scale sediment reworking, mixing or insufficient bleaching (Supplementary Information Section 2). The age estimates were combined with stratigraphic information to develop a Bayesian age model for Layers 7–20 (Fig. 2e and Supplementary Table 6). Details of samples, preparation, measurement, and data-analysis procedures are provided in the Supplementary Information. The age model suggests that Unit I started to accumulate from 374–299 kyr ago (here and below, we give modelled age estimates and total uncertainties at 95.4% probability),

corresponding to the earliest evidence of hominin occupation at the site (Layer 19). The layers containing stone artefacts and wooden implements were dated to from 361–298 kyr (Layer 18) to 286–250 kyr (Layer 10). The topmost layer dated (Layer 7) has a modelled age of 270–220 kyr.

The archaeological component of Layers 10–18 consists of 35 wooden implements (Fig. 3 and Extended Data Fig. 4), numerous lithic artefacts (Extended Data Fig. 3), four antler soft hammers (Extended Data Fig. 10), and a few bones exhibiting anthropogenic cut-marks (Extended Data Fig. 3). Details of each wooden artefact are given in Supplementary Information (Section 3) and Extended Data Figs. 5–9. Only one piece (T1-259) retains some bark (Extended Data Fig. 4d), and 23 items have pointed tips. These are either rounded (Fig. 3b), or chisel-like with a thin, flat blade (Extended Data Fig. 5); or shaped with a ridge towards the point (Extended Data Fig. 7b). Most items are complete in having both ends preserved, unlike the fragmented examples from sites such as Clacton [8] (UK), Florisbad [9] (South Africa), Kalambo Falls [10] (Zambia), Ohalo [11] (Israel), Abric Romani [12] and Aranbaltzar [13] (Spain). Two are self-evident as large digging sticks that would probably require both hands when used (Fig. 3e, 3f; Extended Data Fig. 5) and are similar to ones found at the ca. 171-kyr old site of Poggetti Vecchi, Italy[3]. Other large items (see Extended Data Figs. 4q, w, x and 6) are probably types of digging implements not seen on other sites. The other implements are smaller and likely to have been used in one hand (e.g. Fig. 3a–c; Extended Data Fig. 4a–m, r–v, z). Five pieces form a distinct sub-group: these are hook-like and appear to have been shaped from the base of a trunk and the top of a root; the root part was then shaped to a sharp, round edge that shows wear through use, and could have been used for slicing through roots (see e.g. Figs. 3d, 3h; Extended Data Fig. 4e, 4u). One piece (T2-555, Fig. 3g) is difficult to interpret. It was finely carved into a symmetrical lozenge shape, both tips appear worn, but with a length of only 7.8 cm is too small to use effectively for digging. This piece might have been used as an awl, or for separating root tangles.

Compared to the wooden artefacts found at other sites, GTQ has a much wider range of implements (particularly of small tools). None of the GTQ artefacts is a projectile, unlike the spears and spear tips from Schöningen [1,14], Lehringen [15], Cannstat [16], Bilzingsleben [17] (Germany) or Clacton[18]. Instead, most of the GTQ wooden tools were most likely designed for digging rather than for hunting. Some of them (e.g. Fig. 3e, f and i) are similar to the digging sticks from Poggetti Vechi [3] and Border Cave [19], but most were probably used one-handed (like a dibble or other small gardening tool) for activities such as probing or grubbing. The tips of several implements have starch grains of tuber-rich plants such as *Lilium* (lily), *Sagittaria trifolia* (arrowhead), *Typha orientalis* (bulrush), *Dioscorea alata* and *D. polystachy* (yam), and *Colocasia* sp. (taro) (see Supplementary Information Sections 3 and 10, and Supplementary Table 22, Supplementary Fig. 10).

The stone artefacts comprise cores, flakes and a small number of retouched flake tools. Tools are mostly small scrapers and retouch is extremely fine, with up to 5 detachments along an edge <10 mm long (see Supplementary Information Section 4 and Extended Data Figs. 3a, c and i). The source materials are non-local, i.e., they cannot be found within 5 km of the site. The scarcity of usable raw materials and the lack of large stone tools might be the reason for the dependency of wooden implements in plant food exploitation by the occupants of the site. One soft hammer is an antler segment with percussion damage at both ends (Supplementary Information Section 4 and Extended Data Fig. 10); the other three are pieces of shed antler, with part of the pedicel damaged where it would have touched stone (see Extended Data Fig. 10). These are the earliest known in East Asia.

The hominin occupation of GTQ spans most likely Marine Isotope Stage (MIS) 9 and part of MIS 8, although late MIS 10 cannot be ruled out given the uncertainty in chronology (Figs. 2 and 4). The global oxygen isotope record shows generally warm and wet conditions during MIS 9 and early MIS 8 [20] (Fig. 4b), which is consistent with the faunal and floral evidence from the site (Supplementary Information Sections 6–9). The pollen record (see Fig. 4a and Supplementary Information Section 9) shows a marked decrease in *Quercus* and *Ulmus* and an increase in *Pinus* after Layer 15; this transition was dated to 315–283 kyr. Because pine pollen can be transported over long distances, this increase probably resulted from an expansion of pine forest at higher elevations as a response to global cooling during MIS 9/8 transition (Fig. 4b) but a marsh wetland dominated by Cyperaceae and Gramineae was present on the lake shore. The local environment of the site was probably sub-tropical to tropical throughout its occupation but later changed to a relatively cold environment. The pollen data shows 40 plant families indicative of a warm and humid subtropical climate; these include several types of aquatic vegetation. The macrofossils also indicate a sub-tropical to tropical vegetation that includes several types of trees, lianas, shrubs and grasses (Supplementary Information Section 9). Abundant aquatic or hygrophilous taxa, such as Cyperaceae, Gramineae, *Alisma* and most of the ferns, indicate that the area around GTQ was a swamp or lake.

The large mammal fauna was dominated by cervids (see Supplementary Information Section 6). The presence of *Stegodon, Megatapirus* and *Rhinoceros* in Layers 18–15 (dated to during MIS 9), which were widely distributed in southern China during the Middle and Late Pleistocene, is consistent with a sub-tropical and tropical environment. Numerous types of small mammals are present, suggesting open grassland, shrub and woodland, and thick forest (see Supplementary Information Section 7). These may have been taken by avian raptors or by small mammalian carnivores. Non-mammalian fauna includes frog, snake, box turtle, and several types of birds, notably at least four species of waterfowl (Anatidae), three species of phasianid, a cormorant, an extinct darter, a small grebe, and three raptorial species (see Supplementary Information Section 8). The bird faunal composition and their relative abundances (with an extinct diving duck as the most common) reinforce the reconstruction of a paleoenvironment with

warm temperatures, a variety of shallow water depths under one meter with significant areas of submerged and emergent vegetation, open areas of deeper water (more than 2 or 3 meters deep), and nearby forest for most of the time that hominins utilized the lake margins (see Supplementary Table 17).

Many of the plants represented by macro-remains at GTQ are potential foods for hominins (Supplementary Tables 18 and 19). For example, pine nut (*Pinus*), hazel nut (*Corylus*), kiwi fruit (*Actinidia*), red-berry and black-berry (*Rubus*) and grape (*Vitis*), are nutritiously valuable (Supplementary Information Section 9). As pine nut and hazal nut can be kept a longer time, they could be particularly important in winter when plant food sources were probably rare. The leaves or stems of some herbs, such as Amaranthaceae, Phytolaccaceae and Cucubitaceae, as well as leaves of some ferns are also edible. Because many of these families contain several thousand species, it is not possible to establish precisely which plants might have been used. However, many species of aquatic plants in the Cyperaceae, Gramineae and *Alisma* have edible leaves, seeds or stems, especially sub-soil corms and rhizomes. These could easily have been extracted from the shallow waters and muddy deposits of the lake shore by the digging sticks and grubbing tools found at GTQ in addition to those plants identified from starch grains on the wooden tools.

Our results indicate that hominins utilised the lake-shore in accordance with the rising and falling of the lake level, both seasonally in response to the summer monsoon, and over longer periods in response to climate fluctuations. We propose that hominins made planned visits to the lakeshore and brought with them the tools for digging into the surface of a soft substrate to obtain tubers, rhizomes or corms. This scenario implies considerable foresight by hominins, as well as a detailed understanding of when and which plants, and which parts of plants, were edible. As such, the GTQ assemblage shows the early use of underground storage organs and the importance of plant foods in early hominin diet in a sub-tropical environment.

The GTQ wooden implements are significant in several respects. First, they provide the earliest unambiguous evidence of digging sticks and the exploitation of USO's from the Oriental biogeographic realm of East Asia, and thus document the use of wooden artefacts in a completely different type of environment from Europe or Africa. Second, GTQ presents a previously unknown range of digging tools and complete, small, hand-held pointed wooden tools, and considerably widens our knowledge of early wooden technology. Third, this evidence presents a scenario of early hominin subsistence in sub-tropical and tropical environments that is plant-orientated, in contrast with northern temperate environments such as Schöningen, where the hunting of large mammals is clearly dominant [1,2]. Finally, the evidence from GTQ shows the importance of Palaeolithic artefacts made from organic materials; and the skill

demonstrated in their manufacture offers a clear counterpoint to the apparent “primitive” nature of the stone tools found in East and Southeast Asia[21].

Declarations

Acknowledgements

This project was funded by the Special Subsidy Fund from National Cultural Heritage Administration of China (2014, 2018 and 2019) to J.-H.L, the Discovery Project from the Australian Research Council to B.L. (DP210100717), the CAS Strategic Priority Research Program (XDB26000000) to X.G., J.-Y.G., Y.W., Y.G. and H.S., the Research Grants Council of Hong Kong to S.-H.L. (17307117), the NSFC grants to F.H. (41772174), J.-Y.G. and C.-L.D. (41977380, 41888101) , T.A.S. (41772013) and H.S. (4200020395) the Zhengzhou University grant to X.G. (XKZDJC202006). We thank T. Lachlan, Y. Jafari, Yu-Jie Guo and Xue Rui for assistance with OSL sample preparation, Rui-Ping Tang for assistance with field and laboratory work, Guang Tong for assistance with references, Xu Liu for supporting and coordinating the project, and the members from the local cultural relic authority and other workers taking part in the excavations.

Author contributions

J.-H.L. organised the overall project and conducted analysis on large mammalian fossils. X.G. and J.-H.L. coordinated the research. J.-H.L. R.D. and X.G. conducted wooden implements analysis and R.D. analysed the antler soft hammers. H.S. conducted wood identification. J.-H.L. and J.-Y.G. conducted regional geology and stratigraphic analysis. Q.-J.R. and X.G. conducted lithic analysis. J.-Y.G. and C.-L.D. conducted analysis on palaeomagnetism and sedimentology. Y.-J.H. conducted fossil carpological study. J.L. and S.-F.L. conducted pollen analysis. Y.G. conducted residue analysis on wooden tools. Y.W. conducted analysis on rodent fossils. T.S. conducted non-mammalian fauna analysis. B.L. and S.-H.L. conducted optical dating; F.H. and S.-H.L. conducted ESR/U-series dating. R.D., B.L., J.-H.L. and X.G. wrote the main text with contribution from all the co-authors.

Competing interests. The authors declare no competing interests.

Correspondence and requests for materials should be addressed to X.G. (gaoxing@ivpp.ac.cn), B.L. (bli@uow.edu.au).

References

1 Thieme, H. Lower Palaeolithic hunting spears from Germany. *Nature* **385**, 807-810 (1997).

2 Conard, N. J. *et al.* Excavations at Schöningen and paradigm shifts in human evolution. *J Hum Evol* **89**, 1-17 (2015).

3 Aranguren, B. *et al.* Wooden tools and fire technology in the early Neanderthal site of Poggetti Vecchi (Italy). *Proceedings of the National Academy of Sciences* **115**, 2054-2059 (2018).

4 Yang, L. F. The preliminary study on the original classification and distribution law of lakes on the Yunnan Plateau. *Transactions of Oceanology and Limnology* **1**, 34-39 (1984).

5 Cheng, S.-Y. & Li, Y.-j. Geomorphology of the Fuxianhu drainage basin and its structural implication. *Journal of Geomechanics* **16**, 383-392 (2010).

6 Zhang, X. Y., Gao, F., Ma, B. & Hou, L. P. A preliminary study on the million years ago remains of paleolithic in Jiangchuan, Yunnan. *Thinking* **4**, 51-55 (1989).

7 Liu, J.-H., Zheng, L., Gao, F. & Ji, X.-P. in *Collected works for "The 40th Anniversary of Yuanmou Man Discovery and the International Conference on Palaeoanthropological Studies"* 130-145 (Yunnan Science Press, 2006).

8 Oakley, K. P., Andrews, P., Keeley, L. H. & Clark, J. D. A reappraisal of the Clacton spearpoint. *Proceedings of the Prehistoric Society* **43**, 13-30 (1977).

9 Bamford, M. K. & Henderson, Z. L. A reassessment of the wooden fragment from Florisbad, South Africa. *J Archaeol Sci* **30**, 637-650 (2003).

10 Clark, J. D., Cormack, J. & Chin, S. *Kalambo Falls Prehistoric Site: Volume 3, The Earlier Cultures: Middle and Earlier Stone Age*. Vol. 3(Cambridge University Press, 1969).

11 Nadel, D., Grinberg, U., Boaretto, E. & Werker, E. Wooden objects from Ohalo II (23,000 cal BP), Jordan Valley, Israel. *J Hum Evol* **50**, 644-662 (2006).

12 Carbonell, E. & Castro-Curel, Z. Palaeolithic wooden artefacts from the abric Romani (Capellades, Barcelona, Spain). *J Archaeol Sci* **19**, 707-719 (1992).

13 Rios-Garaizar, J. *et al.* A Middle Palaeolithic wooden digging stick from Aranbaltza III, Spain. *Plos One* **13**, e0195044 (2018).

14 Schoch, W. H., Bigga, G., Böhner, U., Richter, P. & Terberger, T. New insights on the wooden weapons from the Paleolithic site of Schöningen. *J Hum Evol* **89**, 214-225 (2015).

15 Thieme, H., Veil, S., Meyer, W., Moller, J. & Plisson, H. Neue Untersuchungen zum eemzeitlichen Elefanten-Jagdplatz Lehringen, Ldkr. Verden. *Die Kunde* **36**, 11-58 (1985).

16 Wagner, E. *Grosswild Jager im Travertingebiet* Universität Stuttgart, (1995).

17 Mania, D. & Mania, U. Geräte aus Holz von der altpaläolithischen Fundstelle bei Bilzingsleben. *Praehistoria Thuringica* **2**, 32-72 (1998).

18 Allington-Jones, L. The Clacton spear: The last one hundred years. *Archaeological Journal* **172**, 273-296 (2015).

19 d'Errico, F. *et al.* Early evidence of San material culture represented by organic artifacts from Border Cave, South Africa. *Proceedings of the National Academy of Sciences* **109**, 13214-13219 (2012).

20 Lisiecki, L. E. & Raymo, M. E. A Pliocene-Pleistocene stack of 57 globally distributed benthic δ18O records. *Paleoceanography* **20**, PA1003 (2005).

21 Gao, X. Paleolithic cultures in China: Uniqueness and divergence. *Curr. Anthropol.* **54**, S358-S370 (2013).

Methods

Excavation method

Great attention was paid in the excavation to stratigraphic control. Excavated areas were divided into subareas (1 m by 1 m, Extended Data Fig. 1b), and deposits were removed in 10–20 cm spits within stratigraphic units. Three-dimensional spatial information was recorded for all artefacts and animal remains with the ATK system and 'Agisoft Photoscan' program (Extended Data Fig. 1c), and systematic geological sampling was conducted for sedimentological analysis and palaeoenvironmental reconstructions. Wooden relics (including wooden implements) were kept in place and labelled. After taking photos and measurements, wooden relics were wrapped in plastic and stored in purified water. Carbowax (Polyethylene glycol [PEG]) was used as a bulking and consolidating agent for later treatment.

Extensive sieving and flotation were carried out on the site. All the excavated sediments in the cultural layers were marked with the origin of layer and subarea and wet-sieved on the site. These sediments were soaked, stirred and precipitated with water, then filtered through a 0.25 mm sieve to separate macroscopic plant remains. The sediments were then passed through a 0.5 cm mesh to separate out clasts (including stone artefacts), fossils and other remains. 25 litres of these sediment samples were randomly selected from each subarea for sieving through a 0.25 mm mesh to retrieve small mammal fossils. Drone aerial photography was used to show the location of the excavation and the topography surrounding the site (Fig 2a).

Palaeomagnetism

The magnetic polarity of the section was established by collecting 29 orientated bulk samples from T3 at 10–20 cm intervals along the sequences from the GTQ site and underlying terrace. The bulk samples collected were each cut into 20×20×20 mm cubes for palaeomagnetic measurements. All specimens were firstly subjected to subjected to 80 °C and 150 °C thermal demagnetization followed by alternating field demagnetization at peak fields up to 60 mT at 5–10 mT intervals, and then were subjected to stepwise thermal demagnetization up to 610 °C with 13 steps and 10~50 °C temperature increments using the TD-4 thermal demagnetizer. The remanence measurements were made using a 2G-760-R cryogenic magnetometer installed in a magnetically shielded space with a background field of <300 nT. All the experiments were performed in the Palaeomagnetism and Geochronology Laboratory of the Institute of Geology and Geophysics, Chinese Academy of Sciences. Demagnetization results were evaluated by orthogonal diagrams[22], and the principal component direction was computed by means of principal component analysis[23] on a minimum of four consecutive steps using the PaleoMag software[24]. All the samples showed a normal polarity. Based on the biostratigraphy and the OSL and ESR dates (see below) which suggest a late Middle-Pleistocene age for the site, we correlate this magnetozone with the Brunhes Chron of normal polarity, indicating that the age of the excavated deposits is <780 kyr.

Electron Spin Resonance/U-series Dating

Three fragments from a mammalian tooth (GTQ-T4-F12, Supplementary Fig. 7) from the Layer 8 of T4, were analysed using electron spin resonance (ESR) method. Dentine and sediment attached on each side of the enamel tissue (sediment-enamel-dentine geometry) were removed carefully by dental drill. The average thickness of enamel fragment before and after the surface grinding were measured. Over 20 μm of the dentine and sediment sides were removed to eliminate alpha dose contribution. Then the enamel samples were crushed and ground into 100-200 μm powder and divided into 10 aliquots for gamma irradiation. Irradiation were pursued at Pekin University with a calibrated ^{60}Co source and the irradiation doses are 10.7, 19.9, 39.1, 76.7, 148.6, 292.2, 592.3, 1019.0, 1318.0, 1843.0, 2678.0, 4522.0 Gy, respectively. The irradiated enamel aliquots were stored for one month before measurement to eliminate unstable signal in the samples.

The ESR measurement were carried out on a X-band Bruker ER041XG ESR spectrometer at the Institute of Geology, China Earthquake Administration. ESR measurement was performed at the room temperature with the acquisition parameters below: 1mW microwave power, 100 kHz modulation frequency, 0.1 mT modulation amplitude, 5 ms time constant, 20 ms conversion time, 1024 points resolution and 5 scans for each measurement. ESR signal intensity of enamel was extracted from T1-B2 peak-to-peak amplitude and normalized by the weight of aliquot. Each sample was measured four times for checking reproducibility. A single saturation exponential (SSE) function was used to fit the dose response data points to determine the D_e of the enamel sample (Supplementary Fig. 7). The D_e is calculated by extrapolating the dose response curve on to the x-axis, which yields a value of 256 ± 5 Gy.

The uranium-series isotopes in the dental tissues were analysed using a Nu Plasma multi-collector inductively coupled mass spectrometer (MC-ICP-MS) at the Radiogenic Isotope Facility (The University of Queensland). The measured uranium concentration in the enamel and dentine tissue were extremely low (~ 0.02 and ~ 0.1 ppm respectively) (Supplementary Table 7), indicating a weak uranium mobility in the groundwater caused by reduction of soluble U(+VI) to insoluble U (+IV) and followed by precipitation in an anaerobic (reductive) environment. This explains why the wooden tools at GTQ could be well preserved. The corrected U-Th ages of both tissues were 128.5 ± 6.8 kyr and 37.9 ± 2.7 kyr. Since no obvious uranium loss in both tissues was indicated by the $^{230}Th/^{234}U$ ratio, the U-Th ages are considered as the minimum constraint of the fossil age.

The coupled ESR and U-series age of the fossil sample were calculated by US-ESR model with “DATA” program [25]. This model introduces a U-uptake parameter p to describe the uranium uptake history in each dental tissue [26]. For the external dose rate, since the uranium concentration in the dental tissues of fossil sample are extremely low, the beta dose contribution from the dentine is negligible and, hence, only the external dose rate (including beta, gamma and cosmic ray dose rates) from the sediment side was taken into account. Since the sediments attached to the fossil had been removed during excavation, we estimated the sediment dose rate based on the average beta and gamma dose rates obtained from two of the optical samples (GTQ-T4-6 and GTQ-T4-7), both were taken from a depth (1.75 m and 1.9 m, respectively) similar to that of the fossil sample (Supplementary Table 4).

The following parameters were used for dose rate and ESR age calculation of the fossil samples: alpha efficiency 0.13 ± 0.02 [27]; beta attenuation factors were based on Marsh [28]; dose rate conversion factors from Adamiec and Aitken[29]; water content in the dentine and enamel tissues are estimated 5 ± 2% and 0 respectively. No radon loss in the dental tissues were assumed. The early-uptake (EU) and linear-uptake (LU) model ages [30] were calculated to test the model sensitivity of combined ESR/U-series age estimates. A combined U-series-ESR (US-ESR) uptake model [26] and a closed-system U-series ESR model (CSUS-ESR)[31] were also calculated; the latter would give a maximum constraint of the fossil ESR age. The dose rate data and age estimates obtained using different models are summarised in Supplementary Tables 8 and 9. Given the low concentration of U in the fossil, different U-uptake models yielded indistinguishable age estimates at ~288 ka, which is excellently consistent with the four optical ages (from ~240 to ~320 ka) obtained for the sediment from the same layer.

Optical dating

The age of the wooden artefacts was constrained by optical dating [32] of the artefact-bearing sediments. Sediment samples were collected by using stainless steel tubes hammered horizontally into cleaned stratigraphic sections. Sample preparation followed standard procedures as described in previous studies [33]. Potassium-rich feldspar (K-feldspar) grains ranging in size between 90 and 212 μm in diameter were extracted. The separated grains were etched in 10% hydrofluoric acid to remove the alpha-irradiated

surface layer. The time of sediment deposition is estimated by dividing the equivalent dose (D_e, i.e., the radiation energy absorbed by grains since deposition) by the environmental dose rate (the radiation dose received by the grains per unit of time) [32,34]. For D_e determination, the infrared (IR) stimulated luminescence (IRSL) of K-feldspar grains was measured. D_e values for individual K-feldspar grains were determined using a two-step (200 °C and 275 °C) regenerative-dose post-IR IRSL (pIRIR) procedure [33,35,36] and the recently developed standardized growth curve and L_nT_n approaches [37-41] (details are provided in the Supplementary Information Section 2).

The environmental dose rate for K-feldspar grains includes contributions from beta particles, gamma rays, cosmic rays. The external beta dose rate was estimated from beta-counting of dried and powdered sediment samples using a Risø low-level beta multicounter system. The gamma dose rate was measured by in situ gamma spectrometry at each sample location. The cosmic-ray dose rate was calculated by taking account of the latitude, longitude and altitude of the site and the burial depth of each sample[40]. The total dose rate of the K-feldspar grains also includes an estimate of the internal beta dose rate due to the radioactive decay of ^{40}K and ^{87}Rb within the grains. A K concentration of 12 ± 1% and a Rb concentration of 400 ± 100 ppm are assumed [42,43]. The measured beta dose rates were corrected for grain-size attenuation, and the beta, gamma and cosmic-ray dose rates were adjusted for water content (based on the measured field values). Details of sample preparation, D_e determination methods, and environmental dose rate determination are given in the Supplementary Information Section 2.

Code availability. All custom R code used to produce the dating results presented here are available from the corresponding authors on reasonable request.

Reporting summary. Further information on research design is available in the Nature Research Reporting Summary linked to this paper.

Data availability

All data generated and/or analysed during the current study are available from the corresponding authors on reasonable request.

22 Zijderveld, J. D. A. in *Methods in Paleomagnetism* (eds S.K. Runcorn, K.M. Creer, & D.W. Collinson) 254-286 (Elsevier, Amsterdam, 1967).

23 Kirschvink, J. The least-squares line and plane and the analysis of palaeomagnetic data. *Geophysical Journal International* **62**, 699-718 (1980).

24 Jones, C. H. User-driven integrated software lives:“Paleomag” paleomagnetics analysis on the Macintosh. *Computers & Geosciences* **28**, 1145-1151 (2002).

25 Grün, R. The DATA program for the calculation of ESR age estimates on tooth enamel. *Quaternary Geochronology* **4**, 231-232 (2009).

26 Grün, R., Schwarcz, H. P. & Chadam, J. ESR dating of tooth enamel: Coupled correction for U-uptake and U-series disequilibrium. *International Journal of Radiation Applications and Instrumentation. Part D. Nuclear Tracks and Radiation Measurements* **14**, 237-241 (1988).

27 Grün, R. & Katzenberger-Apel, O. An alpha irradiator for ESR dating. *Ancient TL* **12**, 35-38 (1994).

28 Marsh, R. E. *Beta-gradient isochrons using electron paramagnetic resonance: towards a new dating method in archaeology*, McMaster University, (1999).

29 Adamiec, G. & Aitken, M. J. Dose-rate conversion factors: update. *Ancient TL* **16**, 37-50 (1998).

30 Ikeya, M. A model of linear uranium accumulation for ESR age of Heidelberg (Mauer) and Tautavel bones. *Japanese Journal of Applied Physics* **21**, L690-L692 (1982).

31 Grün, R. An alternative model for open system U-series/ESR age calculations: (closed system U-series)-ESR, CSUS-ESR. *Ancient TL* **19**, 1-4 (2000).

32 Huntley, D. J., Godfreysmith, D. I. & Thewalt, M. L. W. Optical dating of sediments. *Nature* **313**, 105-107 (1985).

33 Jacobs, Z. *et al.* Timing of archaic hominin occupation of Denisova Cave in southern Siberia. *Nature* **565**, 594-599 (2019).

34 Aitken, M. J. *An Introduction to Optical Dating*. (Oxford University Press, 1998).

35 Blegen, N. *et al.* Distal tephras of the eastern Lake Victoria basin, equatorial East Africa: Correlations, chronology and a context for early modern humans. *Quaternary Sci Rev* **122**, 89-111 (2015).

36 Thomsen, K. J., Murray, A. S., Jain, M. & Botter-Jensen, L. Laboratory fading rates of various luminescence signals from feldspar-rich sediment extracts. *Radiat Meas* **43**, 1474-1486 (2008).

37 Li, B., Roberts, R. G., Jacobs, Z. & Li, S.-H. Potential of establishing a ‘global standardised growth curve’(gSGC) for optical dating of quartz from sediments. *Quaternary Geochronology* **27**, 94-104 (2015).

38 Li, B., Roberts, R. G., Jacobs, Z., Li, S. H. & Guo, Y. J. Construction of a 'global standardised growth curve' (gSGC) for infrared stimulated luminescence dating of K-feldspar. *Quaternary Geochronology* **27**,

119-130 (2015).

39 Li, B., Jacobs, Z., Roberts, R. G. & Li, S.-H. Single-grain dating of potassium-rich feldspar grains: Towards a global standardised growth curve for the post-IR IRSL signal. *Quaternary Geochronology* **45**, 23-36 (2018).

40 Li, B., Jacobs, Z., Roberts, R. G., Galbraith, R. & Peng, J. Variability in quartz OSL signals caused by measurement uncertainties: Problems and solutions. *Quaternary Geochronology* **41**, 11-25 (2017).

41 Li, B., Jacobs, Z. & Roberts, R. G. Validation of the LnTn method for De determination in optical dating of K-feldspar and quartz. *Quaternary Geochronology* **58**, 101066 (2020).

42 Huntley, D. J. & Baril, M. R. The K content of the K-feldspars being measured in optical dating or in thermoluminescence dating. *Ancient TL* **15**, 11-13 (1997).

43 Huntley, D. J. & Hancock, R. G. V. The Rb contents of the K-feldspars being measured in optical dating. *Ancient TL* **19**, 43-46 (2001).

Figures

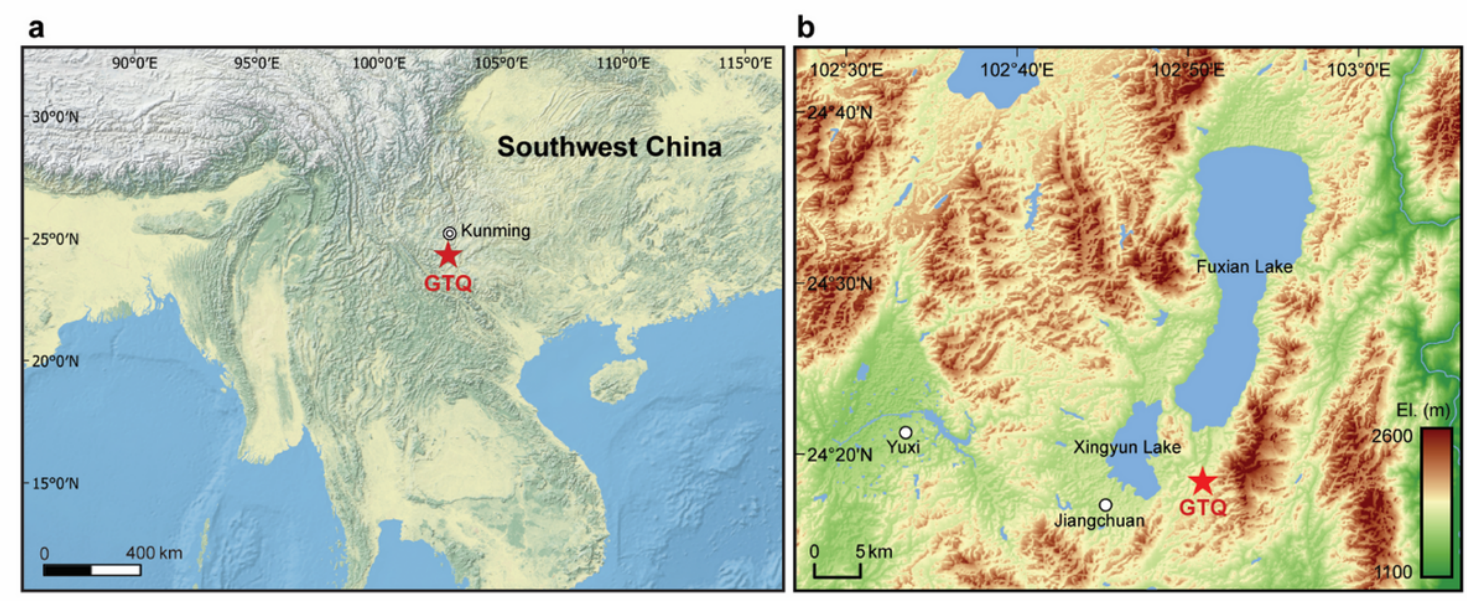

Figure 1

Location of the Gantangqing (GTQ) site in Yunnan province, China. a, Regional map of southeast Asia showing the location of GTQ and the provincial capital city Kunming. b, Digital elevation map (DEM) indicating the GTQ site, Fuxian Lake, Yuxi and Jiangchuan cities and the surrounding area. Note: The designations employed and the presentation of the material on this map do not imply the expression of

any opinion whatsoever on the part of Research Square concerning the legal status of any country, territory, city or area or of its authorities, or concerning the delimitation of its frontiers or boundaries. This map has been provided by the authors.

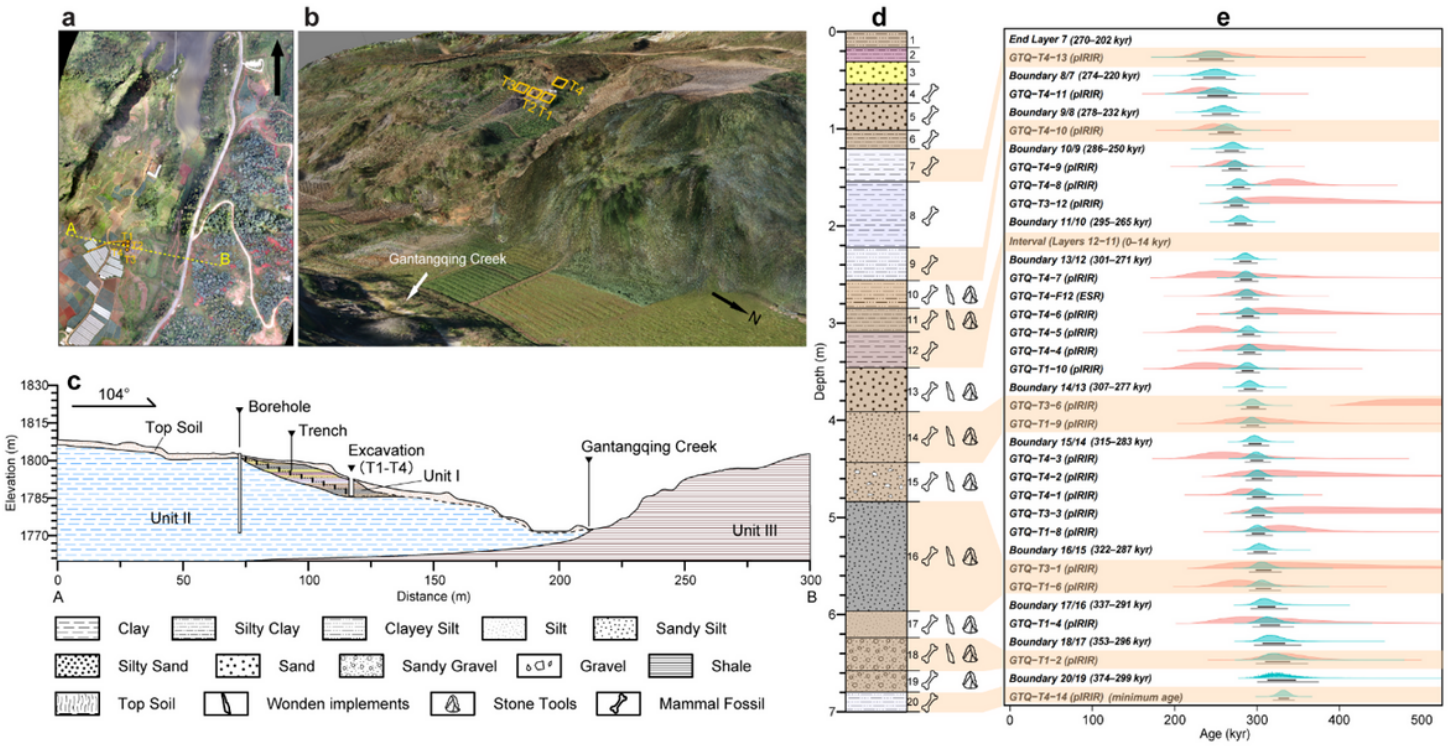

Figure 2

Landscape, stratigraphy and chronology of the Gantangqing site. a, Aerial photograph showing the area surrounding the site and the location of excavation trenches (T1–T4). The cross-section between points A and B is illustrated in panel c. b, 3D model showing the landscape of the site and the locations of T1–T4. c, Schematic model of the stratigraphic cross-section between points A and B in panel a. d, Stratigraphic layers, depth and archaeological contents. e, Bayesian age modeling of optical and ESR dates. Orange probability distributions represent the unmodeled ages (likelihoods), and green distributions represent the modeled ages (posterior probabilities). The narrow and wide bars beneath each distribution represent the 68.2 and 95.4% probability ranges of the modeled ages. Modeled ages for each layer boundary and duration for interval are given in parentheses (95.4% probability).

Figure 3

A selection of wooden implements from GTQ. a, T1-32. a1, Close-up of the sharp tip with two whittling surfaces and one a distinct ridge. b, T2-1677. b1, Whittling marks. c, T2-1676. d, T2-1674. d1, Close-up of the tip, showing the flange at the proximal end, and with scraping marks produced by a chiseled or pointed stone tool. d2, Whittling marks. e, T1-1901. e1, Chisel-like tip with whittling marks. f, T3-73. f1, Chisel-like tip with whittling marks. g, T2-555. h, T2-1667. h1, Close-up view of sharp tip with two whittling surfaces and one distinct ridge. h2, Truncated branch resulting from woodworking. i, T3-124. Each sub-division on the scale = 2cm. Illustrations of other wooden artefacts with close-ups are provided in Extended Data Figs. 4-9.

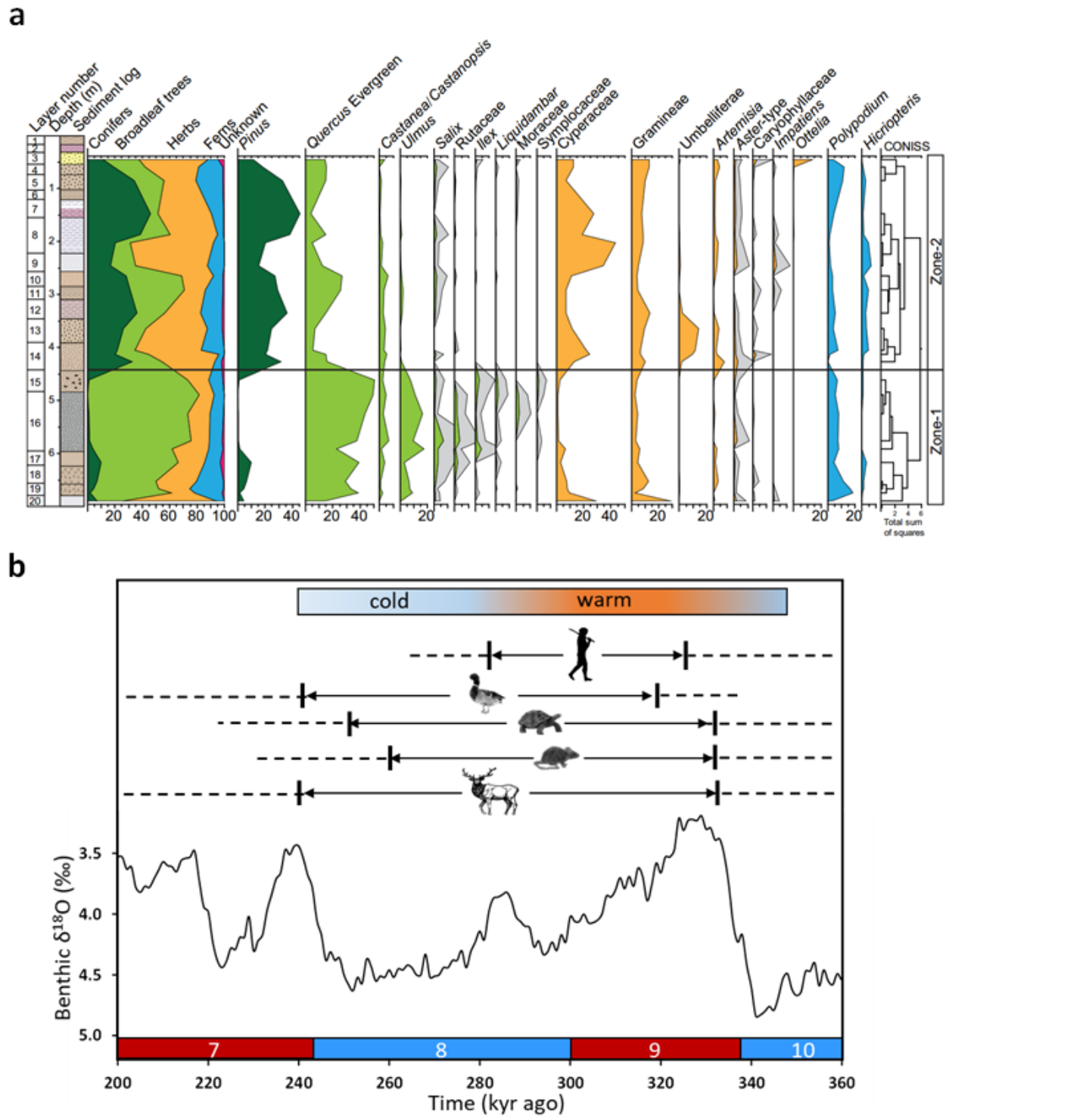

Figure 4

Pollen record and climatic context of the Gantangqing site. a, Composition of main pollen taxa identified in the site. Taxa shown in grey are exaggerated by 5 times. b, Conceptual model showing the climatic and environmental context of the site. The oxygen isotopic record is the LR04 benthic stack δ18O record20. The numbers (7–10) shown in the red and blue bars on the x-axis represent the corresponding marine isotopic stages. The ‘cold-warm’ bar on the top is based on the pollen record shown in a. The horizontal

lines show the time spans of major fauna identified at the site, which are based on the Bayesian model age estimate (Fig. 2e); both ends of the full and dashed lines represent the highest probability density and the 95% probability ranges, respectively.

Supplementary Files

This is a list of supplementary files associated with this preprint. Click to download.

- GTQExtendedDataFigures.docx
- GTQSImasterfile.docx